

Supplementary Materials: Field Observations of Three Mixed Snow Avalanches

Dieter Issler ^{1*}, Peter Gauer ¹, Mark Schaer ² and Stefan Keller ³

Abstract. Three mixed-snow avalanches of widely different sizes, which occurred in the winter 1995 in Switzerland, showed a number of interesting phenomena in an unusually clear fashion. In particular, one could clearly distinguish three deposit types that differed in a consistent way with regard to their location, hardness and density as well as the number and sizes of snowballs embedded in the fine-grained matrix. In addition, there were a wealth of small, and mostly qualitative, observations that can be used to constrain the values of important dynamical parameters of these avalanches if they are combined and analyzed by means of simple models. This document presents the observations made during the fieldwork; the analysis is presented in the main paper “Inferences on mixed snow avalanches from field observations”.

S1. Introduction

This document describes three snow avalanche events with a substantial suspension layer (a.k.a. powder-snow avalanches or mixed avalanches) that occurred in the Swiss Alps between January 10 and February 1st, 1995. The report [1]—available only in German—gave a first account of our field observations, with only a preliminary interpretation of the data. Moreover, when we recently revisited the data, we found some inconsistencies in the maps and estimated numbers that we endeavored to correct in the present document. It serves as the foundation of the analysis and interpretation of our observations in [2].

The reasons for publishing this data after more than two decades are twofold: First, these three events showed important properties of mixed snow avalanches more clearly than any other avalanches we have encountered since, and the observations made on the deposits link to the measurements that have been made in recent years at avalanche test sites such as Vallée de la Sionne and Ryggfönn [3–6]. Second, they demonstrate that much useful information can be gained even without instrumentation by means of field investigations after the event. In this way, it becomes possible to sample a wide variety of avalanche paths to complement measurements at the few existing instrumented sites.

The three avalanches to be described here were of very different size and occurred under different circumstances, but they shared their meteorological origin. In large parts of the Swiss Alps, the snow cover was shallow, spatially variable and generally subject to constructive (temperature-gradient) metamorphism when the first major snow storms of the season 1994/1995 hit between December 31st and January 3rd, and again between January 8 and 11, 1995 [7]. In many places, 1 m of new snow or more was deposited at atypically low temperatures around -10°C and under strong north-westerly to westerly winds. Despite apparently ideal release conditions, only few spontaneous avalanches occurred during or shortly after these storms. One of them was a medium-size avalanche (according to the new EAWS classification of avalanche size [8], which will be used throughout this document), released on or around January 11 from the south-eastern flank of Vilan (2376 m a.s.l.) above the village of Seewis in the Prättigau Valley, eastern Switzerland (Figure S1), see Section S2.

After the storm, continuous strong westerly to south-westerly winds in large parts of the Swiss Alps transported large quantities of new snow to lee slopes. At high altitudes, the temperatures remained below freezing, but they fluctuated strongly around the freezing point at intermediate altitudes (1000–2500 m a.s.l.). Some minor snowfalls at low temperature occurred during this period. Late on January 30, a very large avalanche released from the east flank of Albristhorn (2762 m a.s.l.) 5 km west of the village of Adalboden in the Bernese Oberland. It caused substantial damage in a mature spruce stand, but fortunately did not claim any victims despite the fact that it crossed and buried an open municipal road. During our survey of the avalanche debris on February 1st (Section S3),

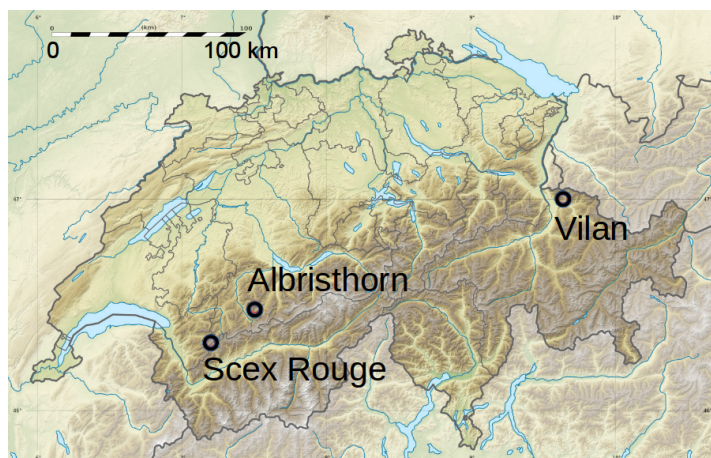
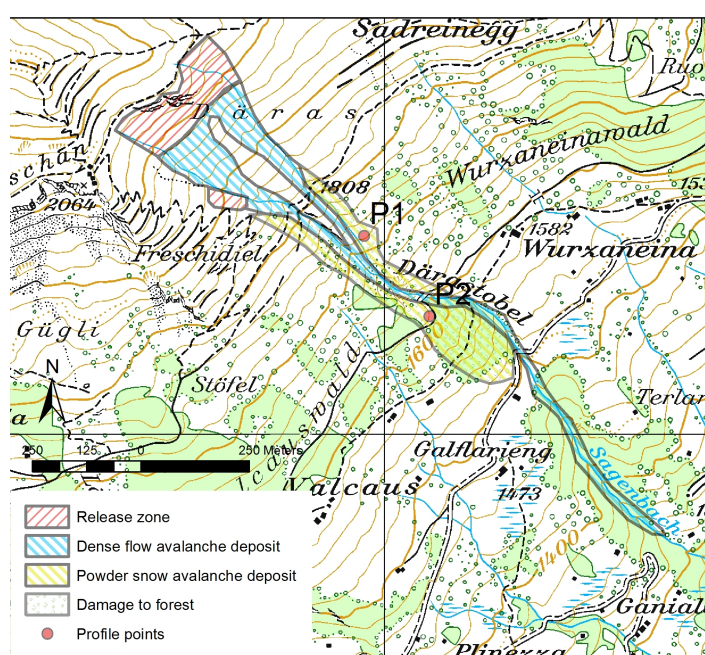


Figure S1. Overview map of Switzerland with the location of the avalanches described in this article. Background map by Wikimedia Commons users Sting and NordNordWest.

Figure S2. Topographic map of the north-eastern flank of Vilan with the release area and trajectory of different parts of the avalanche of 1995-01-11 and the location of two snow pits. Pixmap © 2019 swisstopo, reproduced by permission of swisstopo (JA100118).



an even larger avalanche released from the trough between Scex Rouge (2971 m a.s.l.) and Oldenhorn (3123 m a.s.l.) near Les Diablerets, Canton of Vaud, some 30 km south-west of Albristhorn. The pass road on the counter-slope was open to traffic, but again nobody was in the danger zone when the avalanche deposited 3 m of extremely hard snow (hardness class “knife”) over a length of 800 m on the road (Section S4).

In all three cases, the extent of our field work was severely limited by time constraints, the availability of personnel, poor visibility or winds that did not allow safe access to the release areas. Local observers, cantonal officials and a team from the University of Lausanne supplied us with additional information. These three avalanches provided us with strong evidence that powder-snow avalanches have a more complex structure than we hitherto had believed. Subsequent literature searches revealed that a number of experimental studies had found related aspects of these phenomena [9–13], but have had little impact on the prevailing views of avalanche dynamics and model development. Our studies of the deposits revealed further features of this type of avalanche—and raised a number of additional questions—that do not seem to have been discussed earlier.

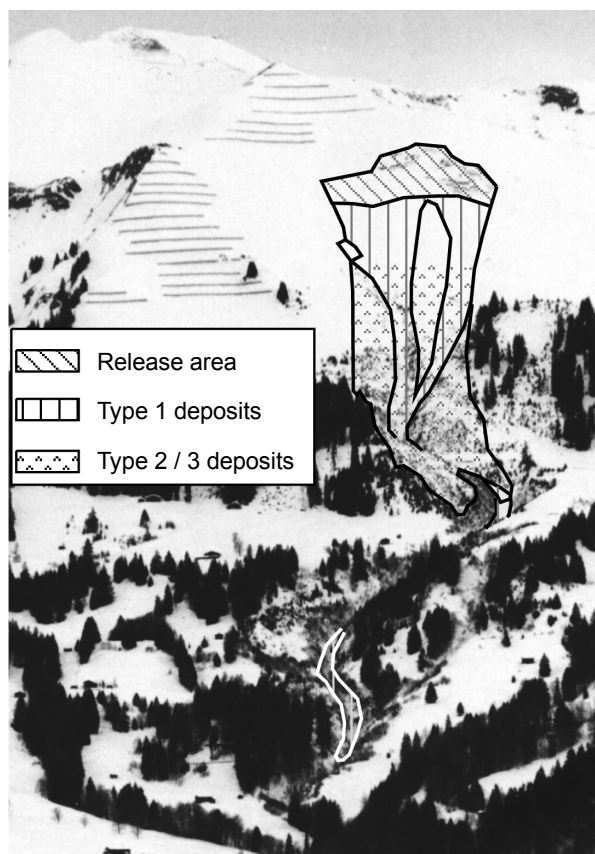


Figure S3. View towards Vilan from south-east. The release area is near the rock face to the right and below the uppermost row of steel bridges. The Däras gully and the surrounding clearing in the forest are visible below. At the first turn of the gully, the powder-snow part separated from the dense-flow part and swept over the more gently inclined area outside the gully.

S2. The avalanche at Mt. Vilan (Seewis, Grisons)

S2.1. Weather and topography

Avalanches release almost annually in the Däras gully on the south flank of Vilan, both as dry-snow and wet-snow avalanches. Reported events with a significant powder-snow component occurred in 1951, 1968 and 1984 (J. Hartmann, personal comm., Seewis, 1995), indicating a return period of 10–20 years for events of similar magnitude as in 1995. This is compatible with the absence of a dense forest stand along the path of the powder-snow avalanche.

In all likelihood, the 1995 avalanche released at the end of the storm on January 11 because no fresh snow was found on top of the avalanche debris. By then, the snow depth at the Weissfluhjoch station, located 500 m higher and some 20 km to the south-east, had increased by about 1.0 m since the storm began. Given the regional gradient of snowfall intensity, the altitude difference and the exposure of the release area to blowing snow, we estimate the average (vertically measured) release height to 1.0–1.5 m. This is in fair agreement with the average release depth (normal to the slope) of 1 m, estimated during a survey flight (S. Margreth, personal communication, January 1995). Due to intensive snow transport, the density of the released slab presumably was around 150 kg m^{-3} , despite the low temperatures. Further down the path, we may assume a density and new-snow height around 100 kg m^{-3} and 1.0 m, respectively.

Prior to the snow storm, the snow cover was between 0.2 and 0.5 m deep in the Prättigau area. It had been exposed to intermittent rain up to high altitudes and to prolonged strong temperature gradients. Therefore, the old snow was slightly humid and contained ice crusts at some places. It consisted mainly of faceted crystals, with occasional depth hoar crystals. In contrast, the new snow consisted of rounded grains about 0.2 mm in diameter at the time of our survey one week after the release.

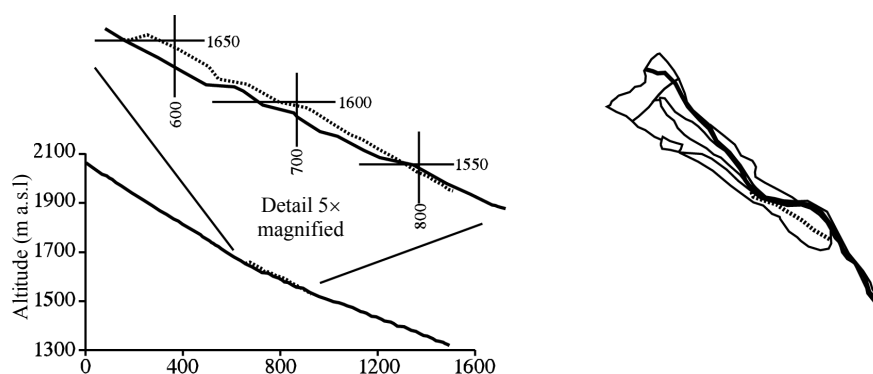


Figure S4. Characteristic profiles of the Vilan avalanche, with the inset showing the difference between the paths of the dense-flow part (thick line) and the suspension layer (dotted line).

The release zone, located between 1980 and 2060 m a.s.l., is between 30° and 40° steep and has an area of slightly less than 3 ha ($3 \times 10^4 \text{ m}^2$). Thus the release volume was in the range 25'000–35'000 m^3 and the mass 3–4.5 kt ($3\text{--}4.5 \times 10^6 \text{ kg}$).

Over the first 600 m, the avalanche track has a fairly constant inclination of 30°. Two 5–10 m wide ravines apparently had already channelized the slowest parts of the avalanche where they merge at 1657 m a.s.l. and form the Däras gully. The latter is 10–30 m wide, 5–20 m deep and has a fairly uniform inclination of approx. 20° (Figure S4). Between 1640 and 1620 m a.s.l., it changes direction from SE to E (see Figure S5), and then again back to SE between 1580 and 1540 m a.s.l.

S2.2. Deposit characteristics

The avalanche debris showed two strikingly different types of texture: On the one hand, the deposit along the gully was distinctly granular, consisting mostly of rounded snow balls up to 10–20 cm in diameter, with some fine-grained snow in the interstitial space (henceforth designated as type 1 deposit). It exhibited remarkably sharp lateral boundaries and a slightly convex surface at many places (Figure S5). On the other hand, the deposit outside the gully bottom consisted mostly of fine-grained snow, with snow blocks dispersed on the surface where the terrain is not too steep (type 2 deposit). Some of the snow blocks were larger (up to 30 cm) than the largest snow balls we found on the surface of the type 1 deposit, but they were much less numerous (and perhaps not as well rounded), see Figure S6. The prevailing flow direction was clearly discernible thanks to small bushes that looked like combed in one particular direction, or flow marks at the surface itself, as if the snow cover had been scoured. Moreover, this direction coincided everywhere with the expected flow direction of a high-speed avalanche.

The morphological features of the type 1 deposit appear to be compatible with a dense, relatively slow flow. The edge of a highly agitated flow could hardly be as sharp as it was the case here, and one would expect substantial run-up along the outer bank of the gully at the bends, which we did not observe. The type 2 deposit has opposite characteristics, and also its visual appearance is strongly suggestive of a high-speed, low-density flow in which the air flow also plays a role. However, the presence of a fair number of rather large particles makes it problematic to identify it simply with the

Table S1. Estimated mass balance of the 1995 Vilan avalanche.

	Volume (10^3 m^3)	Mass (10^6 kg)
Release area	25–35	3–5
Type 1 deposit	10–20	3–8
Type 2 deposit	5–10	1–2
Net erosion along path		0–7



Figure S5. View of the uppermost turn of the Däras gully. In the upper part of the image, one sees the confluence of the two main ravines. The powder-snow part frequently sweeps over a larger width, as the trim line shows. The type 1 deposit is clearly visible along the centerline of the gully and begins substantially above the bend.

relic of a powder-snow cloud, by which we understand a dilute flow of air and small particles kept in suspension by the air turbulence. We will therefore use the term “non-dense flow” temporarily.

We found type 2 deposits as far up as about 300 m from the release area. In the lower track, this flow had a width of 50–100 m while type 1 deposits were confined to the gully. The sharp bend of the gully around 1630 m a.s.l. (S5) played a pivotal role in the investigation of this avalanche event: The type 1 deposits were still confined to the center of the gully, while the type 2 deposits continued in an essentially straight line. The steep gully bank, which is only partially visible on the left side of Figure S5, showed a large degree of erosion, but no flow marks that would indicate significant superlevation of the flow associated with the type 1 deposit. The path of the avalanche part responsible for the type 2 deposit could be traced along the side of the Däras gully over a distance of 300–400 m from the bend, thanks to the damage it had inflicted on the vegetation (Figure S7). Unfortunately, lack of time did not allow for accurate mapping of the perimeter of the type 2 deposit. Very roughly, we estimate the mass of the type 2 deposit downstream of the bend to about 1 kt, based on the balance of erosion and deposition indicated in Table S1. The uncertainty is very large, however, because this number is the difference of two numbers of similar size with large uncertainties.

A similar “phase separation” also occurred on the north-eastern edge of the avalanche. A sharp trim line visible in the upper right corner of Figure S5 indicates that high-speed avalanches pass over this pronounced shoulder often enough to prevent a dense, mature forest stand from developing. The deposit on the north-eastern side of the gully had similar properties as the one on the south-western side.

The spruce needles and twigs served as tracers that discriminate clearly between undisturbed new snow and the type 2 avalanche deposit, which otherwise might be hard to distinguish, having the same grain types and sizes. We dug two snow pits at the points P₁ (1720 m a.s.l.) and P₂ (1630 m a.s.l.) marked in Figure S2, both with clear type 2 deposits. P₁ was near the left margin of the avalanche,



Figure S6. Snow pit at location P₂. The old snow layer at the bottom consisted of faceted crystals and goblets; there are no embedded fir twigs and needles. The new snow layer of approx. 1 m was completely eroded. The snow layer above the old snow is a type 2 deposit, with embedded snow balls and fir twigs throughout its entire depth. Behind the pit, snow balls up to 0.3 m in diameter are visible in their original location; they are sintered to the snow surface.



Figure S7. Damage to trees caused by the 1995 Vilan avalanche. The photo was taken at approx. 1630 m a.s.l. on the SW-side of the Däras gully.

P₂ in the area with most pronounced vegetation damage, to the right of the Däras gully and a short distance downstream of the upper bend. Figure S6 shows the pit at P₂, and Figure S8 schematically presents the layering we found at the two points.

At P₁, the old-snow layer was between 20 and 30 cm deep, followed by new snow of similar depth, consisting of small rounded grains only, without any tracers. The avalanche debris on top consisted of a similar matrix, but contained tracers that delineated a sharp and fairly regular boundary to the new snow layer underneath. The snow balls on the surface were fairly small, from hazelnut to egg size. Careful probing with the fingers revealed that small snow balls, distinguished by their elevated hardness, were also embedded inside the type 2 deposit layer. In contrast, no such particles could be individuated in the new-snow layer.

The new-snow layer was completely absent at P₂, i.e., it was eroded in its entirety by the non-dense flow. The old-snow layer was only 15–20 cm deep, but we cannot determine with reasonable certainty whether it was shallower from the start than at P₁ or was partly eroded. The type 2 debris layer varied from 30 to 50 cm in depth and thus was typically about twice as thick as at P₁. Its texture showed the same fine-grained matrix with embedded tracers and snow balls, whose sizes ranged to more than 10 cm, however. The largest snow blocks on the surface exceeded the size of a human head, had a mass of up to 5 kg and considerable strength when we divided them with a spade. With the naked eye, we

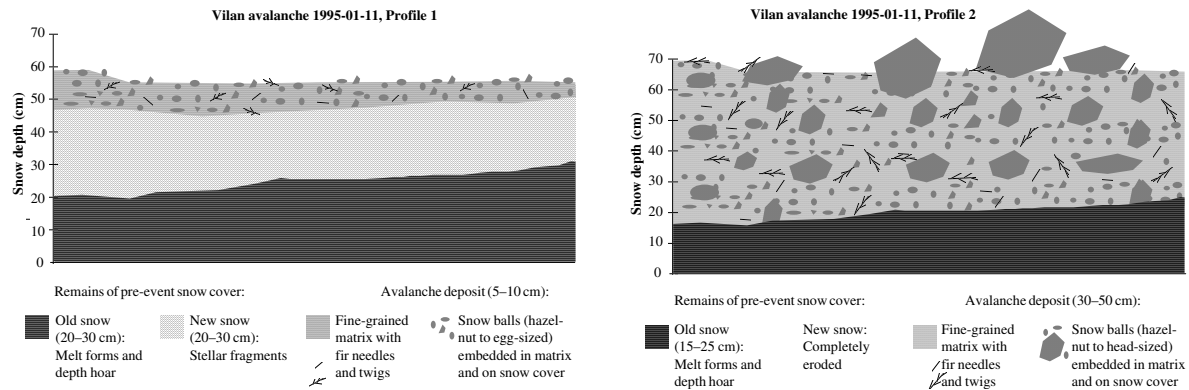


Figure S8. Schematic representation of the snow pits at the points P₁ (top) and P₂ (bottom), which are located in the area of type 2 deposits of the Vilan avalanche. At P₁, part of the new-snow layer remained, with its original texture intact and no embedded snow balls or fir needles. The deposit above the new-snow layer is thin and contains only small embedded snow balls and some organic material. At P₂, the avalanche debris is directly on top of the old-snow layer and contains larger snow balls.

could not discern any internal structure. and they did not contain any needles or twigs. The snow balls were sintered to the deposited layer. We do not know whether this was mainly the result of warming that had occurred since the avalanche release or due to the pressure at impact. The surface texture of the snowballs and of the debris layer suggests that a suspension flow (powder-snow cloud) persisted after the snow balls were emplaced, but it is not clear whether that flow eroded or deposited snow.

S2.3. Damage pattern, pressure and mass balance

The flow associated with the type 2 deposit (designated as type 2 flow henceforth) must have developed quite rapidly. Already at 1800 m a.s.l., it broke branches and twigs from young spruce trees growing between the two stream channels (there was no vegetation at higher elevation that would be damaged by avalanches other than full-depth flows). Further downhill, larger branches and entire trunks up to 20 cm in diameter were broken and carried along by the avalanche. The forest damage was limited, however, because avalanches are too frequent for a dense stand to grow up in the path (see Figure S7). We did not observe any damage below 1600 m a.s.l., where the vegetation is dominated by very flexible deciduous bushes. Based on the damage pattern, we roughly estimate the pressure exerted by the type 2 flow to 1–3 kPa, not only near the snow surface, but also at 3–5 m above it. The Däras gully itself is devoid of vulnerable vegetation so that we cannot estimate the pressure exerted by the type 1 flow.

Along the Däras gully, the type 1 flow progressively lost mass and stopped at altitude 1320 m a.s.l., after a distance of about 1 km from the beginning of the gully, despite the path inclination still being approximately 20°. A rough estimate of the deposit volume in the gully—based on the measured length, average width and estimated average depth—gives 10'000–20'000 m³. At an average estimated density of 300–400 kg m⁻³, this corresponds to 3–8 kt and indicates that in all likelihood the type 1 flow eroded a significant amount of snow. The entrainment ratio, defined as the final deposited mass divided by the release mass, was between 1 and 2, thus considerably lower than in the majority of the smaller avalanches at Monte Pizzac (Dolomites, Italy) studied by Sovilla *et al.* [14].

S3. The avalanche from Albristhorn (Adelboden, Bernese Oberland)

S3.1. Weather and terrain

The Albristhorn avalanche released some two weeks after the major snow storm from January 8 to 11 and near the end of the following prolonged period with strong westerly winds, intermittent minor snow falls and generally higher temperatures. Due to this, the snow cover in the run-out zone

Figure S9. Overview map of the Albristhorn avalanche of 1995-01-30 near Adelboden, Bernese Oberland. Spacing of the grid lines is 1 km, equidistance is 20 m. Pix-map © 2019 swisstopo, reproduced by permission of swisstopo (JA100118).

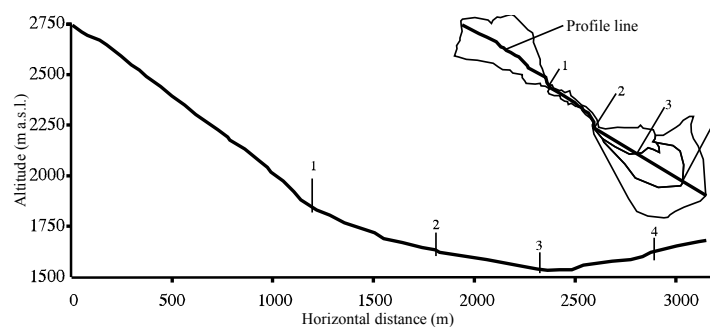
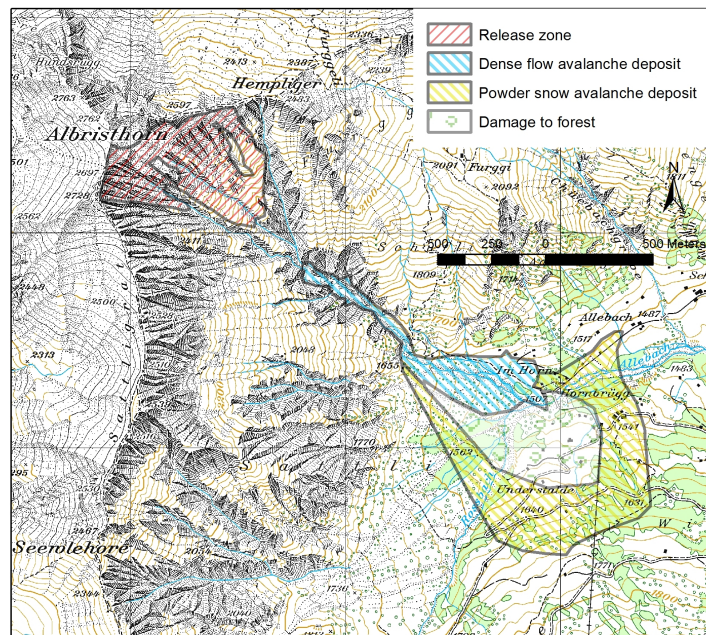


Figure S10. Albristhorn avalanche, terrain profile along the line indicated in the inset.

and presumably also in the lower track was humid. The release occurred towards the end of such a snow fall: At locations not reached by the avalanche, the new-snow layer was about 15 cm deep while the avalanche debris was covered by 3 cm of new snow. At altitudes from 1500 to 1800 m a.s.l., the snow cover just prior to release thus consisted on average of approximately 1 m of old snow and 10–15 cm of new snow. The old-snow layer contained fairly large faceted crystals and a significant fraction of melt forms; apart from buried crusts, its hardness was a low 1 (“fist”) on the hand-test scale. The new-snow layer consisted mostly of small rounded grains, and its density varied between 200 and 230 kg m⁻³. Melt forms were also mixed in, presumably indicating that there had been episodes of snow drift between snow falls.

The release area of this very large avalanche comprised a substantial part of the very rugged, semi-circular bowl that forms the south-eastern flank of Albristhorn. The crown length was approx. 1.3 km, the aspect varying from east to south-west (Figs. S9–S12). While the crown was clearly visible, the location of the staunchwall must be estimated. We think it most likely that it was around 2300 m a.s.l. in the easternmost part and between 2400 and 2500 m a.s.l. in the central and southernmost part. The release area would then amount to 25–30 ha, rather than the 35 ha we estimated originally [1]. The triangular area immediately beneath the summit has an inclination between 30° and 35°, which increases to 40° in the deeply furrowed region further down. Despite the sharp ridges between furrows, we are led to assume that the avalanche essentially released as a single slab because there was no indication of lobes from separated flow episodes in the dense-flow deposit; moreover, it appears

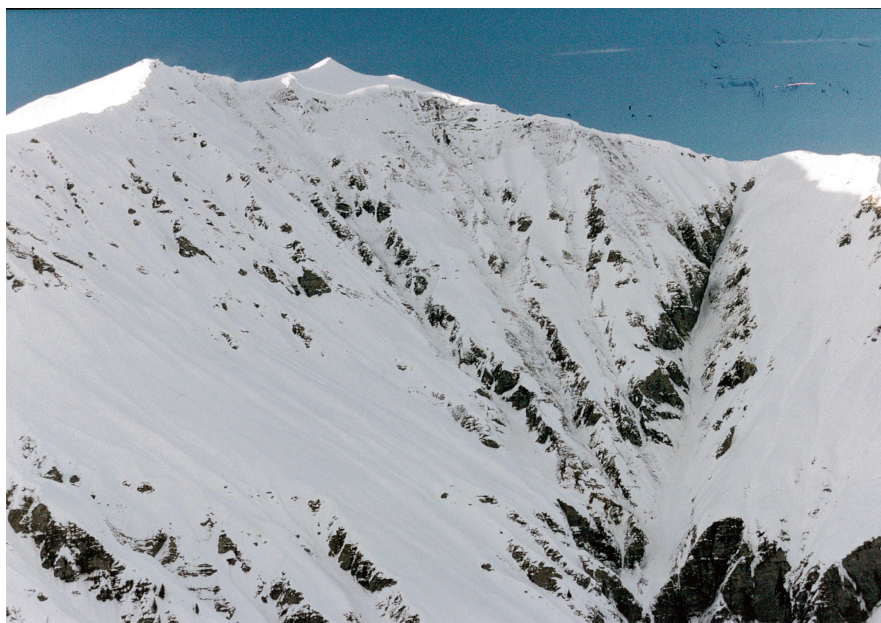


Figure S11. Release area of the Albristhorn avalanche of 1995-01-30 seen from the east.

unlikely that the powder-snow cloud would have become so powerful if there had been a sequence of smaller releases.

Immediately below the release area, the gullies channelize the avalanche rapidly. The gullies merge at 1900 m a.s.l. and form a deep, narrow, winding and irregular gorge, with a mean slope angle of 23° over 650 m (Figure S13). At 1620 m a.s.l., the gorge opens onto an alluvial fan with an average slope of 10° over 650 m. At 1500 m a.s.l., the fan terminates beneath the approximately 20 m high south-eastern bank of the Allebach torrent flowing NNE. Beyond the bank, the terrain ascends gently, but with increasing inclination towards south-east. Open grassland dominates in the lower parts whereas mature spruce stands with a sinuous boundary are more prevalent higher up. Mature spruce with typical trunk diameters of 30 cm or more cover the river bank densely. In 1995, there was a T-bar lift starting from a wooden shed near the edge of the river bank. Several vacation homes on the lower part of the slope face Albristhorn. At the western end of the alluvial fan, a small bridge crosses Allebach.

The avalanche deposit consisted of two clearly distinguishable zones, the proximal one sharing many features with the type 1 deposit of the Vilan avalanche and the more distal zone being similar to the type 2 (non-dense) deposit of the Vilan avalanche. In addition, the type 2 deposit of the Albristhorn avalanche exhibited a gradual change along the flow direction with regard to depth and particle content. The most distal parts of the deposit were devoid of embedded particles; it will be convenient to refer to them as type 3 deposits.

The type 1 deposit in the proximal zone stretches from the confluence of the gullies at 1900 m a.s.l. to close to the river bank, with its tip 10 m in front of the mentioned bridge. The total area of this zone is 17–18 ha. The deposit showed the typical features of a humid dense-flow avalanche (Figure S14): a sharply defined perimeter, considerable deposit depth, high snow density, granular structure with partly rounded snow clods with a wide range of sizes, a very rugged surface due to faulting and thrusting, with a multitude of shear planes, many of which are close to vertical. The dense flow was in the process of turning east to follow the line of steepest descent along Allebach when it stopped. It appears to have been too slow to run up against the river bank. It was not practical to walk on this part of the deposit, to dig snow pits or to probe its depth due to the very irregular surface and the hardness of the deposit. From our observations near the front and the photos from the helicopter survey flight, we originally estimated an average snow depth of approximately 3 m in this zone, but had to revise this to approximately 2 m in the light of an improved mass balance estimate (see below). We do



Figure S12. Fracture crown of the Albristhorn avalanche near the summit, viewed from helicopter.

not know whether some of the original snow cover remained intact underneath the avalanche, but consider this unlikely in view of the softness of the snow cover and the considerable shear stress that the avalanche masses must have developed. If these assumptions and estimates are correct, the type 1 deposit volume is about $3.5 \times 10^5 \text{ m}^3$. Measuring the density of this very hard deposit (5, “knife”) with irregular hollows proved to be difficult; in the snow blocks, we obtained values around 600 kg m^{-3} . We believe $400\text{--}450 \text{ kg m}^{-3}$ to be a fair estimate for the average deposit density of the dense flow. The deposited mass then lies in the range 120–180 kt.

The type 2 and 3 deposit, in contrast, was found on and beyond the river bank and ascending the counter-slope to about 1750 m a.s.l. It widened from the apex of the alluvial fan with an opening angle of approximately 60° . In addition, a branch extended some 300 m to the east along Allebach. The total area of the type 2 and 3 deposit is around 85 ha, its depth diminishing from 20–30 cm near the edge of the dense-flow deposit to less than 1 cm in the most distal parts; the average over the entire zone was between 5 and 10 cm. Density measurements, which were possible only where the deposit thickness was at least 5 cm, gave values close to 400 kg m^{-3} . It is possible that the density was lower in the thinner deposits in the more distal areas, but they do not influence the average very much. With these assumptions, we find the combined mass of the type 2 and 3 deposit in the range 18–32 kt, or approximately 10–20% of the total deposit mass.

One could easily distinguish the deposit of the non-dense flow from the new-snow layer because the snow grains were sintered together, the hardness being in the range 3–4 (“finger” to “pencil”) and the density varying from 400 to 440 kg m^{-3} . Even near the distal edge of the deposit, where its thickness was less than 1 cm, its hardness was still clearly higher than the hardness of the new snow below and above. Some melt-form grains were also embedded in the otherwise fine-grained layer. As in Seewis, we could individuate snow balls of various sizes embedded in the fine-grained matrix by probing the deposit layer with the fingers. Their hardness and density were in the range 4–5 (“pencil” to “knife”) and $460\text{--}500 \text{ kg m}^{-3}$, respectively. Both their number and their maximum size diminished in the distal direction. Again as in Seewis, the largest snow balls were found on the surface of the deposit, sintered to it. We did not see similar particles on top of the dense-flow deposit.

The largest particles measured 25 cm in diameter and were found only on the valley floor and 100–200 m beyond the river bank, i.e., to an elevation 30–50 m above the lowest point. At the distal end of the deposit, snow balls were absent, i.e., the flow consisted of a pure suspension layer at that altitude. Due to the gradual decrease in particle size and number with distance, it is difficult to indicate



Figure S13. View down the strongly channelized track of the Albristhorn avalanche.

a boundary between the snowball-laden type 2 deposits and the particle-free type 3 deposits. A reasonable estimate is about 15–20 ha for the type 2 deposits and about 65–70 ha for the type 3 deposit.

S3.2. Mass balance

The fracture depth along the crown could only be estimated from the helicopter—with large uncertainty because reference scales were missing. Beyond doubt, however, the spatial variability was large. Near the summit, the fracture depth (measured normal to the ground) was approximately 3 m (Figure S12) while the minimum values were about 0.5 m. We believe the average to have been between 1 and 1.5 m. The average over the entire release area is likely somewhat smaller, but presumably not less than 1 m. We thus estimate the release volume to $(3\text{--}4) \times 10^5 \text{ m}^3$. Considering the settling time of two weeks, warming and wind compaction, the average density was hardly less than 200 kg m^{-3} . Thus our estimate of the release mass comes to 60–90 kt.

From our observations, we can establish a rough mass balance for this avalanche event, differentiating between the three different types of deposit that we identified (Table S2). The difference between the release mass and the total of the deposit mass must be due to erosion and entrainment. The uncertainty in our estimate being large, we indicate the most likely range. Measuring the potential erosion area, we can estimate the mean erosion depth if we assume that our measured density values from the deposit area are representative for the entire path. Note that the area occupied by the dense-flow deposit has to be considered a potential erosion area. The same holds for the deposit area of the non-dense flow, but our snow pits indicated that very little erosion had occurred on the counter-slope.

From the simple fact that the entrainment depth is limited by the availability of erodible snow, one obtains constraints on parameters that we could not measure directly. In particular, we found the depth and density of the dense-flow deposit to be overestimated in the original report. The main results that can be read from the table are the following: (i) The total deposited mass was two to three times the release mass. (ii) The mass fractions of the type 1, type 2 and type 3 deposits were approximately 0.85, 0.1 and 0.05 (iii) The mass fraction of the type 2 flow may be somewhat underestimated because it may have deposited some mass on the alluvial fan before the type 1 flow arrived and overflowed or entrained it again. (iv) The avalanche eroded most of the erodible snow cover along its path—in the track and the gorge as well as on the alluvial fan.



Figure S14. View onto the upper part of the deposit of the dense-flow part between points 2 and 3 of the profile line shown in Figure S10.

S3.3. Damage patterns and pressures

Due to lucky circumstances, there were no victims and only very little material damage to structures. Some falling trees narrowly missed the houses in their vicinity. The shed of the T-bar lift withstood the avalanche, but the wooden door, located on the western side of the shed (obliquely exposed to the avalanche flow) was damaged and pushed into the room. However, there was substantial damage to the forest. The potential forest damage area, defined as the total area spanned by the polygon formed by the farthest trees with severe damage, amounts to nearly 50 ha from the apex of the alluvial fan to an altitude of 1600 m a.s.l. on the counter-slope. Only a small fraction of this area is actually forested so that only about 2 ha of forest were destroyed or severely damaged. Most of the damage occurred in the mature, dense spruce stand on the river bank, see Figure S15. These trees were felled by the type 2 and/or type 3 flow—the type 1 flow stopped briefly before the river bank. Some trees were broken well above ground, but the majority were uprooted. From this observation only, it is difficult to determine which flow type caused most of the damage.

Surprisingly, single trees with trunk diameters above 30 cm were also broken in dense, healthy stands substantially farther away from the alluvial fan (and beyond the type 2 deposits). In those cases, break points several meters above the ground left no doubt that the suspension layer (powder snow

Table S2. Estimated mass balance of the 1995 Albristhorn avalanche. The release and deposit volumes are estimated from the survey data and photos. They were converted to mass estimates assuming a snow cover density of 200 kg m^{-3} and using the measured or estimated deposit densities indicated in the text. Net erosion is based on the difference between released and deposited masses, the corresponding volume is calculated from the assumed snow cover density. The erodible snow cover is estimated from the overflowed area below the stauwall, the estimated snow depth and snow cover density.

Zone	Volume (10^3 m^3)	Mass (10^6 kg)
Release volume/mass	300–400	60–90
Type 1 deposit	300–400	120–180
Type 2 deposit	30–50	12–22
Type 3 deposit	15–25	6–10
Net erosion	250–750	50–150
Erodible snow cover	350–500	70–100



Figure S15. Main damage area of the 1995 Albristhorn avalanche viewed from helicopter. The ski lift shed that suffered light damage is visible in the upper center.

cloud) is to blame for this damage. The fact that only isolated trees were broken indicates that the stagnation pressure was close to the threshold for breaking such trees and that the pressure varied strongly in space (and also in time), as is expected in a highly turbulent flow. Zones of elevated stagnation pressure had typical widths of 20–50 m.

This avalanche event was due to the combination of circumstances favorable to avalanche release—the weak old-snow layer, the intense snow storm in mid-January and the unusually long period of intense winds from the same direction—that do not conspire often. Yet it probably cannot be considered an extreme event for this location because both the release area and the average release depth could be larger still. The spruce trees that were destroyed had trunk diameters of 30 cm or more and an age of 50–100 years. The avalanche of 1946 (Figure S16) presumably was only a little smaller than the 1995 event, but there is no report on forest damage. On the one hand, we may assume that these were the only events of that size in the 20th century, else there would be further reports. On the other hand, there are only bushes and low pine trees to be found on the alluvial cone, suggesting that the frequency of avalanches reaching that area is high enough to prevent a spruce stand from growing up. From these indications, we estimate the return period of the 1995 event to be 50–200 years.

S4. The avalanche from Scex Rouge (Les Diablerets, Vaud)

The avalanche that descended from the north-western flank of Scex Rouge and the wide cirque between Scex Rouge and Oldenhorn on 1995-02-01 towards noon was the largest avalanche of that winter (and perhaps even of the period 1985–1998) in Switzerland. Over a distance of more than 800 m, it completely buried the Col du Pillon road that traverses the counter-slope 60–80 m above the valley floor (Figure S17), but fortunately nobody was in the danger zone during the event. Time constraints and dubious weather conditions limited us to a visual survey of the avalanche track from the pass road on the counter-slope and a study of the type 2/type 3 deposits above the pass road. We received important supplementary information from eye witnesses, the police, SLF's local observer, employees of the ski area and telepherique company, and from the University of Lausanne.

Schoeneich [15] summarizes complementary investigations of this avalanche, focused on the release area, the type 1 deposit, and climatological questions. On 1981-12-15, an even larger event destroyed the forest that had existed before and even cleared the avalanche path of large boulders. This circumstance prevented the 1995 event from causing more extensive damage. In a consulting report, Meister [16] described that event and estimated the return period of events of like size as in 1995 to about 30 years. The climatological study of Schoeneich [15] arrived at similar results.



Figure S16. Descent of a powder-snow avalanche from Albristhorn on 1946-01-02 around noontime. The 1995 event was presumably somewhat larger and more powerful than the 1946 event. Photo reproduced with permission from Bildpress AG, Bern, Switzerland, 1946.

S4.1. Weather and topography

The meteorological conditions closely resemble the ones that led to the Albristhorn avalanche. The Scex Rouge glacier to the south-east of the release area must have been the source of large quantities of snow that stormy south-westerly winds deposited in the release area after the snow storm of January 10–14. A snow pit profile, taken 2.5 km to the east of the release area under comparable topographical conditions only one hour before the release, gave no hint of the imminent danger (F. Schallenberg, personal comm., February 1995). The day after, a snow pit profile by the same experienced observer immediately above the 3 m high fracture crown clearly showed unfavorable layering. However, the release might have been triggered by an over-snow vehicle removing snow in front of the rope-way station. Repeated attempts to artificially release further avalanches in the area on the day after the event were unsuccessful.

Eyewitness reports differed widely (from a few seconds to ten minutes) in their estimate of the interval between the two avalanches that descended along different paths, first from the cirque between Scex Rouge and Oldenhorn, and then from the north-western flank of Scex Rouge. Based on reports received, Issler *et al.* [1] estimated the total release area to exceed 1 km². Our reanalysis showed, however, that a substantial part of that area is not steep enough for avalanche release. Moreover, the eastern extension of the primary release area is rather uncertain. The two release areas—separated by a prominent shoulder—measure about 30–35 ha and 20–25 ha, respectively (Figure S17). The fracture depth was up to 3.4 m, and in large parts of the release areas the failure plane was close to the ground. This leads to an estimated 1.5–2 m average fracture depth (vertically measured) and release volumes (masses) of $(5\text{--}7 \times 10^5 \text{ m}^3)$ (100–150 kt) and $(3\text{--}5) \times 10^5 \text{ m}^3$ (60–100 kt), respectively.

S4.2. Deposits

The path and deposit of the type 1 flow could to some degree be reconstructed from the visible traces. In the primary avalanche, it was strongly channelized when it flowed out of the trough Dar Dessus, precipitated over the cliff at 2000 m a.s.l. and then followed an S-shaped path imposed by the topography, turning sharply towards west at Creux du Pillon. A similar channeling occurred from

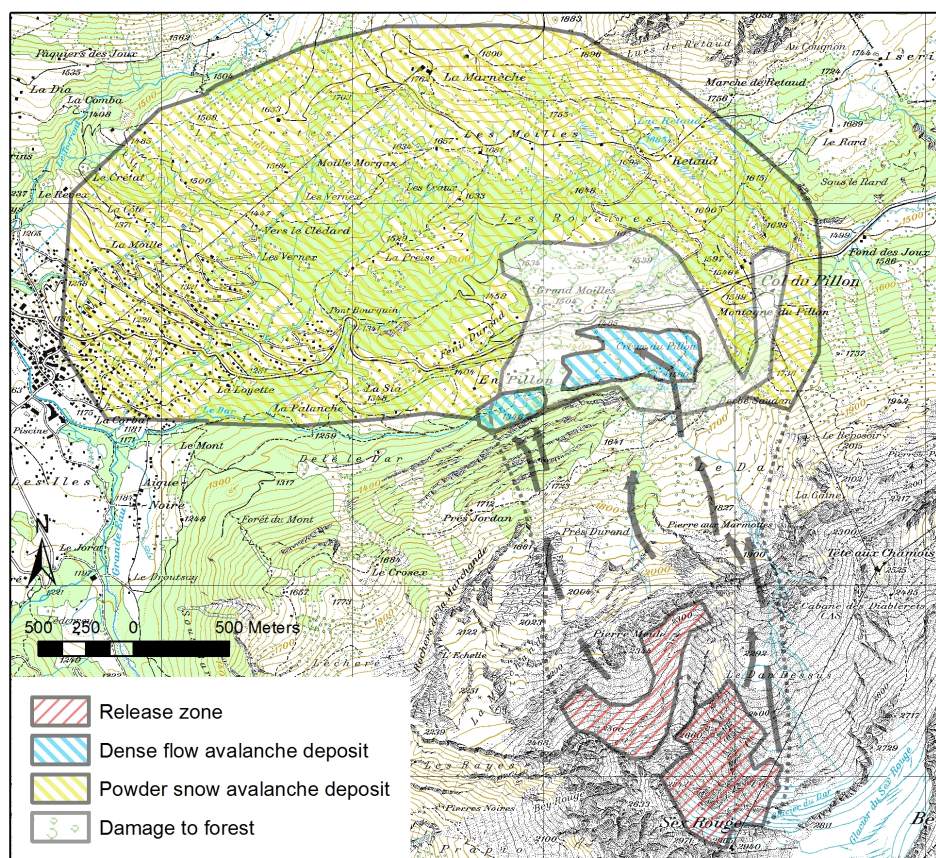


Figure S17. Release area and approximate path of the 1995 Scex Rouge avalanche. The suspension layer reached the village of Les Diablerets at the western edge of the map. Spacing of grid lines is 1 km, equidistance is 20 m. Pixmap © 2019 swisstopo, reproduced by permission of swisstopo (JA100118).

the secondary release area to Pierre Meule. Between 2000 and 1800 m a.s.l., the flow direction of those masses changed from north-west to north so that they collided with the primary avalanche in the deposit zone. Much of the snow eroded along the path was humid and cohesive so that characteristic pressure ridges and fault planes developed (Figure S19). Both the abrupt deflection of the primary flow and the collision with the secondary flow must have dissipated a large fraction of the kinetic energy, shortening the run-out towards west. The westernmost snow masses from the secondary release area followed a fairly straight path, falling over several cliffs and forming the westernmost part of the deposit without colliding with the primary avalanche. The type 1 deposit area totals approximately 20–25 ha; with the maximum deposit depth of about 12 m and an estimated average of 5 m, the type 1 deposit volume and mass are near or even exceed 10^6 m^3 and 500 kt, respectively.

Type 2 and type 3 flow. With a fall height of up to 1500 m, several pronounced cliffs along the track and the rather steep ascent on the counter-slope, it is not surprising that the suspension layer reached a height of at least 200 m at the valley floor, estimated both by eyewitnesses and from Figure S20. Photos taken when it reached Les Diablerets (about 3 km to the west) show it to be at least 400 m high, but it had lost all its power by then and only produced a light snow fall. The deposit area was far too large to be mapped during our brief survey; the outermost boundary indicated in Figure S17 is therefore rather speculative. The eastern boundary, however, was more readily recognizable because a branch of the type 2 and/or type 3 flow crossed the saddle of Col du Pillon and felled a few scattered trees even near the téléphérique station. However, topographical considerations show that these masses cannot have originated from the cirque between Scex Rouge and Oldenhorn; more likely, they originate from a tertiary release from the north flank of Tête aux Chamois (not shown in the map Figure S17). Such a tertiary release might also reconcile the conflicting timing indications we have received.



Figure S18. View from the pass road to the release area, with the summit of Scex Rouge to the right. A part of the snow masses from the secondary release flowed around the cliff in the lower middle. The main part of the avalanche flowed through the channel visible higher up and fell over the cliff.



Figure S19. View from the pass road onto the run-out zone of the Scex Rouge avalanche. The shear planes in the foreground may be due to the collision of two branches of the avalanche.



Figure S20. View of the suspension layer flowing down the main valley, seen from the Scex Rouge ropeway station, at a few meters from the fracture crown. Photo by Markus von Siebenthal, Feutersoey, Switzerland.

When the main mass of the type 2/type 3 flow impacted on the steep counter-slope, which is inclined $35\text{--}40^\circ$, a part was deflected to the west and flowed along the valley floor. Most of it, however, ascended about 100 vertical meters to the plateau of Grand Moilles and eventually turned west towards Les Diablerets. The total area overflowed by the suspension layer was $3\text{--}6\text{ km}^2$. We have no measurements of the type 3 deposit depth; given the enormous area and the barely noticeable snowfall at Les Diablerets, we estimate the average deposit depth as 1–2 cm, giving a type 3 deposit volume of $(0.3\text{--}1.2) \times 10^5\text{ m}^3$ and a corresponding mass of 15–60 kt.

The available photos of the powder snow cloud afford a rough consistency check of these estimates. The cloud volume in Figure S20 is of the order of $1 \times 0.5 \times 0.2\text{ km}^3 = 10^8\text{ m}^3$. Its visual appearance suggests a volumetric particle concentration between 10^{-4} and 10^{-3} . The corresponding ice volume of $10^4\text{--}10^5\text{ m}^4$ corresponds to a mass of 10–100 kt.

We estimate the area of type 2 deposits to $0.3\text{--}0.6\text{ km}^2$. On the pass road, the type 2 deposit was up to 3 m deep, due to the geometry of this incision in the slope profile. On the plateau of Grand Moilles, we measured values ranging from 0.2 to 0.5 m, diminishing with distance from the release area. This leads us to estimate the average deposit depth over the entire type 2 deposit area to 0.3–0.4 m. All samples of the deposit density yielded values near 500 kg m^{-3} . The total mass of the type 2 deposit then most likely was in the range 65–130 kt or about 10–25% of the total deposit mass.

The snow pits we dug at several locations around Grand Moilles largely confirmed our findings from the Vilan and Albristhorn avalanches. We lack data on the local quantity of new snow at Grand Moilles, and at most pit locations there were not enough tracers like fir needles to clearly mark the boundary between deposit and undisturbed snow cover. Therefore we cannot assess the erosive power of this avalanche reliably. However, at some pit locations it appeared that all the new snow was eroded.

Table S3. Estimated mass balance of the 1995 Scex Rouge avalanche assuming a density of 200 kg m^{-3} in the erodible snow cover. See Table S2 for further explanations.

Zone	Volume (10^3 m^3)	Mass (10^6 kg)
Release area	800–1200	160–250
Type 1 deposit	800–1200	350–600
Type 2 deposit	100–250	65–130
Type 3 deposit	30–120	15–60
Net erosion	1200–3500	180–630
Erodible snow cover	1000–3000	200–600

If this is indeed the case, it is significant because the new-snow layer was wet and hard to erode due to the high temperatures before the event.

Our density measurements yielded $500\text{--}550 \text{ kg m}^{-3}$ in the type 2 deposit, or about twice the value of the old-snow layer from the major snowstorm in mid-January. Some settling may have occurred since the event due to high temperatures and absorption of long-wave radiation. Over a large area around Grand Moilles, small snow balls were embedded in the deposit. Larger clods up to 30 cm in diameter were sintered to the surface, as in the case of the other two avalanches—however, 100 m above and 500 m away from the valley floor in this case. Their density was around 600 kg m^{-3} or 10–20% higher than that of the type 2 deposit.

S4.3. Mass balance

The uncertainties in the mass balance are large: The mapping of the release area is not very precise, the location of the stauwall is not known, the average release depth must be guessed from the values measured along the crown, there are no measurements in the track, and only rough estimates of the deposit depth of the dense flow are available (Table S3). Combining the upper limit of the release mass with the lower limit of the deposited mass, an entrainment ratio of only 1.13 results; in the other extreme, it would be nearly 4. However, a value of 2–3 appears most plausible. The relative uncertainty is largest for the type 3 deposit, but this is relatively insignificant for the total mass balance. Our best estimates indicate that the type 2 and type 3 flows together accounted for 15–30% of the total mass, with 20–25% considered most likely—in agreement with the values found at Albristhorn.

Comparing our estimates of the net erosion with the erodible snow mass along the path, we conclude that well over half of the available snow was eroded in this event. A potentially significant observation is that the type 2/type 3 flow seems to have eroded much of the (relatively thin) new-snow layer while climbing up the steep slope to Grand Moilles and running out on the plateau. As explained above, this inference is only tentative, but observations made at the test site Vallée de la Sionne right before and after the 1999-02-10 event support it: The non-dense part of that avalanche eroded nearly 2 m of new snow in the vicinity of the observation bunker on the counter-slope 50 m above the valley floor.

S4.4. Damages and pressure distribution

The type 2/type 3 flow buried the pass road over a length of nearly 1 km up to 3 m deep. The deposit enclosed branches up to 10 cm in diameter. At least at one location, a large stone flying uphill bent the massive steel railing of the road. It is likely that more such damage would have occurred, were it not for the 1981 event that transported boulders up to 1 t up this slope and largely cleared the path of forest and movable boulders. In contrast to 1981, there was only minor damage to the cabins at Grand Moilles in 1995. However, the poles of the power and telephone line were pulled out of the ground or broken over a distance of 400 m between Grand Moilles and the summit of the pass road. Only a few dozen trees were felled in 1995, but the damage area extended to about 1600 m a.s.l. (200 m above the valley bottom) and 300 m north of the pass road.



Figure A1. Photos of the Vilan avalanche. The *upper left* photo was taken some distance uphill from the location of snow pit P₂. It shows a clear trimline separating the unaffected forest stand from the avalanche path where most trees were damaged to some degree. The remaining three pictures were taken near the location of snow pit P₂. *Upper right*: On the left side of the Däras gully, there is a similarly sharp trimline. *Lower left*: Debris from trees was lying on the surface and fine snow partially covered the snow clods over large parts of the type 2 deposit. *Lower right*: Fir trees in the path were typically 10–20 years old and sustained different types of damage (see also photos on the left), but were not transported away completely. This suggests that the avalanche pressure was not far above the strength of the tree trunks.

Appendix A Selected photographs from the 1995 avalanches

Appendix A.1 Vilan

The images in Figure A1 contain a significant amount of qualitative information, none of which is novel, but all of which can be useful for corroborating our views of the responsible processes. Our main observations are the following:

- On both sides of the path, sharp trimlines can be seen. Damage from the 1995 avalanche extends all the way to the trimline (at least on the western, orographically right-hand side).
- Nearly all fir trees in the path sustained damage if they were taller than approximately 2 m and no longer flexible enough to reduce the avalanche load through bending. Some trees were uprooted, others were broken some distance above the snow surface. However, only relatively small tree tops or branches were transported over substantial distances, not entire trees. This suggests that the torque exerted by the avalanche was not far above the bending strength of the tree trunks.
- Over large parts of the type 2 deposits, there was a thin layer of fine-grained snow covering the snow clods, but not small branches and fir twigs. This can be due to either residual snow fall after the avalanche event or the rear part of the powder-snow cloud passing over the type 2 deposit and depositing onto it.

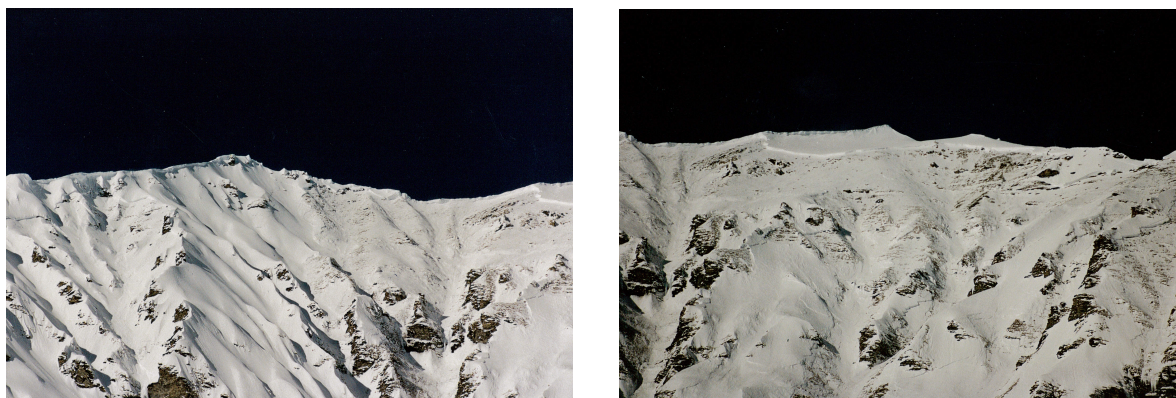


Figure A2. Partial views of the release area of the Albristhorn avalanche.



Figure A3. Close-up view of parts of the release area of the Albristhorn avalanche. The fracture propagated over a very long distance across pronounced ridges. Note that erosion in some areas involved all of the old snow from before the snow storm around January 10, 1995, whereas the sliding plane remained within the snow cover in other places.

Appendix A.2 Albristhorn

Most of the available information on the release area was obtained from the photos taken during a helicopter flight. Due to the prevailing winds, it was not possible to land safely near the summit of Albristhorn and to perform measurements.

The photos collected here show the surprising extent of the release area (Figure A2) and that the fracture propagated across sharp ridges that would normally bound an avalanche release (Figure A3).

Appendix A.3 Scex Rouge

The selected photos are from the pass road, where the avalanche had already ascended some 60 m above the valley floor (Figure A4) and from the plateau Grand Moilles, more than 100 m above the valley floor (Figs. A5 and A6).

The damage on the railing (Figure A4, right panel) is intriguing because it cannot be due to a car hitting the post. Mere snow clods do not have sufficient momentum and hardness to bend an H-shaped steel post. If the culprit was a rock transported by the avalanche, its size must have been considerable because it presumably hit the post at an oblique angle (the pass road rests on a nearly vertical and several meters high wall). Strangely, the upper railing is bent mostly near the post. There was no rock visible nearby, but it may have been deposited higher up and buried in the snow or been removed when the road was cleared. Meister [16] reports, however, that rocks with a mass up to 1 ton were carried up to the pass road in the large 1981 event.



Figure A4. Traces of the deposit of the non-dense part of the Scex Rouge avalanche on the pass road after it was cleared. The railing was probably hit by a rock transported by the avalanche. Rocks up to 1 ton reached the road in the 1981 event.



Figure A5. Damaged trees and avalanche debris at Grand Moilles, more than 100 m above the valley floor on the opposite slope.



Figure A6. *Left:* A snow clod sintered to the deposit surface. *Right:* Trench through the snow cover on the plateau north-west of the cabins at Grand Moilles. The red rope shows the interface between the undisturbed snow cover and the deposits. The width of the spade is approx. 20 cm.

At Grand Moilles, the damage was moderate. Most cabins remained undamaged or sustained minor damage on chimneys and other protruding elements, but branches, tree tops and loose material were transported over considerable distances (Figure A5, left panel). The boundary between severely damaged trees and unscathed ones was rather sharply delineated (Figure A5, right panel). Somewhat surprisingly, the low-voltage power line running parallel to the valley in the vicinity of the cabins was damaged over an extended distance. Despite the small cross-sectional area of the poles and their considerable strength, many were either broken or pulled out of the ground.

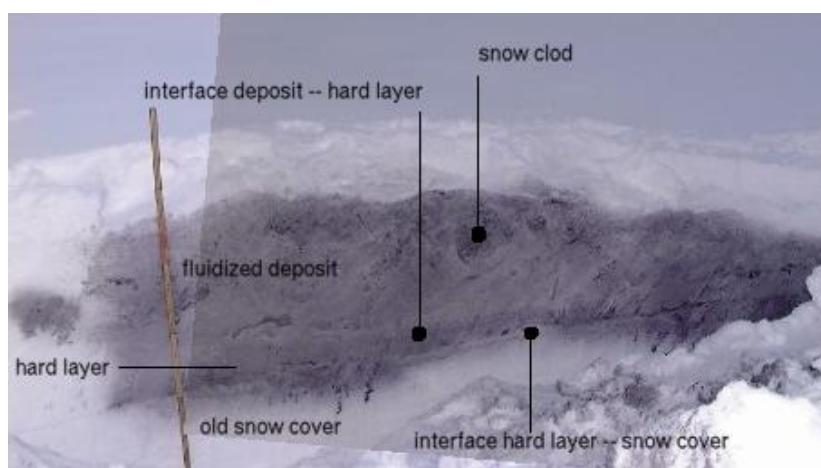


Figure A7. Avalanche at Inneralp, Davos area, Switzerland, February 2004. The trench is oriented perpendicular to the flow direction in the very distal area of the deposits of the non-dense flow. The exposed cross-section was sprayed with an ink–alcohol mixture to make the deposit texture visible. The deposit tapers off towards the flow boundary on the right-hand side. Photo: H. Gubler.

Appendix B Miscellaneous observations from other avalanches

In this appendix, we present selected unpublished observations from 14 other avalanche events in 11 different paths, collected during the winters 2004–2006 in the Davos area, Switzerland, as far as they are relevant to the analyses presented in [I]. More extensive reports are accessible at the website <http://snf.ngi.no>, see Table A1.

Table A1. List over avalanche events discussed in Appendix B with URL that contains more detailed reports. The estimated size, S is indicated in terms of the Canadian Avalanche Size Classification, which primarily relates to avalanche mass, M , through $M = 10^S$ tons.

Nr.	Path	Size	Type	Date	Report URL
1	Inneralp	3+	dry	2004-02-24	http://snf.ngi.no/inneralp.040224.html
2.1	Breitzug	4	wet	2004-01-13	http://snf.ngi.no/breitzug.040113.html
2.2	Breitzug	4	wet	2005-02-12	http://snf.ngi.no/breitzug.050212.html
2.3	Breitzug	4	dry/wet	2006-03-13	http://snf.ngi.no/breitzug.060313.html
3	Taferna	4–	dry	2005-02-07	http://snf.ngi.no/taferna.050207.html
4	Salezertobel	4	humid	2005-02-13	http://snf.ngi.no/salezertobel.050213.html
5	Dorfberg	4	wet	2005-03-20	http://snf.ngi.no/dorfberg.050320.html
6	Rüchitobel	4–	dry	2006-01-18	http://snf.ngi.no/reports/report_Ruechitobel_2006-01-18.pdf
7.1	Gotschnawang	3.5	dry	2006-01-20	http://snf.ngi.no/reports/report_Gotschnawang_2006-01-20.pdf
7.2	Gotschnawang	3.5	dry	2006-03-12	http://snf.ngi.no/gotschnawang.060312.html
8	Kreuzweg	2	dry	2006-01-24	http://snf.ngi.no/kreuzweg.060124.html
9	Drusatscha	3.5	dry	2006-02-14	http://snf.ngi.no/drusatscha.060214.html
10	Sertig Dörfli	4	dry	2006-02-21	http://snf.ngi.no/reports/report_Sertig_2006-02-21.pdf
11	Chaiseren	4.5	mixed	2006-03-10	http://snf.ngi.no/reports/report_Chaiseren_2006-03-10.pdf

Two of the three events in the Breitzug path (2.1, 2.2) were wet-snow avalanches when they arrived at the run-out zone, though they most likely started as dry-snow avalanches. The third event 2.3 and the Salezertobel avalanche 4 also started as dry-snow avalanche and became humid along the path. The only pure wet-snow avalanche was the Dorfberg avalanche 5. The remaining avalanches can be characterized as dry-snow avalanches throughout. At Gotschnawang, avalanches 7.1 and 7.2

were released artificially to secure ski runs, and the Drusatscha and Chaiserer avalanche were likely released by skiers or snowboarders. The remaining avalanches occurred spontaneously.

We observed longitudinal grading of the deposit in the avalanches 1, 3, 6, 7.1, 7.2, 9, 10, and 11.

A trench dug perpendicular to the main flow direction in the deposit of the Inneralp avalanche 1 provided an example of lateral grading of a type-2 deposit (Figure A7).

Author Contributions: See the main paper for a list of author contributions.

Funding: See the main paper for funding information.

Acknowledgments: See the main paper for the list of persons to whom the authors are indebted for their help and discussions.

Conflicts of Interest: The authors declare no conflict of interest. The funders had no role in the design of the study or interpretation of data, in the writing of the manuscript, or in the decision to publish the results.

References

1. Issler, D.; Gauer, P.; Schaer, M.; Keller, S. Staublawineneignisse im Winter 1995: Seewis (GR), Adelboden (BE) und Col du Pillon (VD). Internal Report 694, Eidg. Institut für Schnee- und Lawinenforschung, Davos, Switzerland, 1996. (in German)
2. Issler, D.; Gauer, P.; Schaer, M.; Keller, S. Inferences on mixed snow avalanches from field Observations. submitted for publication.
3. Barbolini, M.; Issler, D., Eds. *Avalanche Test Sites and Research Equipment in Europe – An Updated Overview*, number D8 in SATSIE Project Deliverables. SATSIE Project Team, 2006. Contributions by T. Jóhannesson, K. M. Hákonardóttir, K. Lied, D. Issler, P. Gauer, M. Naaïm, T. Faug, L. Natale, M. Barbolini, F. Cappabianca, M. Pagliardi, L. Rammer, B. Sovilla, K. Platzer, E. Suriñach, G. Furdada, F. Sabot and I. Vilajosana.
4. Gauer, P.; Issler, D.; Lied, K.; Kristensen, K.; Sandersen, F. On snow avalanche flow regimes: Inferences from observations and measurements. Proc. of the Intl. Snow Science Workshop ISSW '08, Whistler, B.C., Canada. International Snow Science Workshop, 2008, pp. 717–723.
5. Sovilla, B.; Schaer, M.; Rammer, L. Measurements and analysis of full-scale avalanche impact pressure at the Vallée de la Sionne test site. *Cold Regions Sci. Technol.* **2008**, *51*, 122–137, doi:10.1016/j.coldregions.2007.05.006.
6. Sovilla, B.; McElwaine, J.N.; Louge, M.Y. The structure of powder snow avalanches. *C. R. Phys.* **2015**, *16*, 97–104, doi:10.1016/j.crhy.2014.11.005.
7. SLF. Schnee und Lawinen in den Schweizer Alpen, Winter 1994/95. Winterbericht 59, Eidg. Institut für Schnee- und Lawinenforschung, Davos Dorf, Switzerland, 1996. (in German)
8. European Avalanche Warning Services. Avalanche size. Available online: <https://www.avalanches.org/standards/avalanche-size/>. (Accessed on 10 October 2019).
9. Schaerer, P.A.; Salway, A.A. Seismic and impact-pressure monitoring of flowing avalanches. *J. Glaciol.* **1980**, *26*, 179–187. doi:10.3189/s0022143000010716.
10. Shimizu, H.; Huzioka, E.; Akitaya, E.; Narita, H.; Nakagawa, M.; Kawada, K. A study on high-speed avalanches in the Kurobe canyon, Japan. *J. Glaciol.* **1980**, *26*, 141–151, doi:10.3189/s0022143000010686.
11. McClung, D.M.; Schaerer, P.A. Characteristics of flowing snow and avalanche impact pressures. *Ann. Glaciol.* **1985**, *6*, 9–14, doi:10.1017/s0260305500009897.
12. Gubler, H.; Hiller, M.; Klausegger, G.; Suter, U. Messungen an Fließlawinen. Zwischenbericht 1986. Mittlg. No. 41, Eidg. Institut für Schnee- und Lawinenforschung, Davos, Switzerland, 1986. (in German)
13. Bozhinskiy, A.N.; Losev, K.S. The Fundamentals of Avalanche Science. Mittlg. 55, Eidg. Institut für Schnee- und Lawinenforschung, Davos, Switzerland, 1998.
14. Sovilla, B.; Somnavilla, F.; Tomaselli, A. Measurements of mass balance in dense snow avalanche events. *Ann. Glaciol.* **2001**, *32*, 230–236, doi:10.3189/172756401781819058.
15. Schoeneich, P. Dépendance météorologique des avalanches du versant Chaussy-Para et du massif des Diablerets. Project report, Inst. de Géographie, Université de Lausanne, Lausanne, Switzerland, 1995. (in French)
16. Meister, R. Lawinengefahr und Lawinenhäufigkeit im Gebiet der Luftseilbahnen Les Diablerets. Expertise G 82.70, Eidg. Institut für Schnee- und Lawinenforschung, Davos, Switzerland, 1982. (in German)